ELSEVIER

Journal of Crystal Growth 208 (2000) 546–554

JOURNAL OF CRYSTAL GROWTH

www.elsevier.nl/locate/jcrysgro

Growth habit of rutile and α-Al_2O_3 crystals

Wen-Jun Li*, Er-Wei Shi, Zhi-Wen Yin

Shanghai Institute of Ceramics, Chinese Academy of Science, Shanghai 201800, People's Republic of China

Received 17 March 1999; accepted 27 July 1999
Communicated by S.R. Coriell

Abstract

The growth habits of TiO_2 and α-Al_2O_3 crystals are observed on the synthetic crystals in the hydrothermal or glycothermal solutions by means of TEM and ED analysis. It is concluded that the habit of α-Al_2O_3 crystal should be the hexagonal platy $\{0\,0\,0\,1\}$ with the $\{1\,1\,\bar{2}\,3\}$ faces; the growth habit of rutile is an elongated prism, bounded by $\{1\,1\,0\}$, $\{1\,0\,0\}$ and $\{1\,0\,1\}$ forms. These results are successfully explained by a new rule concerning growth habit proposed by Wen-Jun Li et al. (J. Crystal Growth, 1999, to be published). Moreover, the growth habit of rutile is related to the concentration of precursor ($TiCl_4$ solution). When the concentration of $TiCl_4$ solution increases from 0.25 to 1 mol/l, the morphology of particles is changed from prismatic form to elongated prismatic form. Its habit change is analyzed through the study of the growth mechanism of rutile.

Keywords: Growth habit; Rutile; α-Al_2O_3

1. Introduction

The growth habit of crystals is mainly determined by the relative growth rates of various crystal faces bounding the crystal, which is dependent on internal structure factors of a given crystal and external conditions such as temperature, concentration of precursor and pH value of solution, etc. Therefore, an explanation of the growth habit of oxide crystal must start from studying the growth mechanism of the crystals. The theoretical models concerning crystal growth habit mainly include the BFDH law [1] and the PBC theory [2]. However, these models only consider the effect of interior structure factors on growth habit, entirely ignoring the effect of exterior conditions on growth habit. Hence, the growth habit of crystal obtained by these theories tends to be not in good agreement with the observed growth habit. For example, for α-Al_2O_3 crystal, according to the PBC theory [3–6], The habit of corundum crystals is rhombohedral $\{\bar{1}\,0\,1\,2\}$. This is not in agreement with the observed platy $\{0\,0\,0\,1\}$ growth forms. Mackrodt [7] allows the effect of surface relaxation on equilibrium crystal morphology to be examined. It is concluded that the habit of α-Al_2O_3 crystal should be rhombohedral $\{\bar{1}\,0\,1\,2\}$ with small $\{0\,0\,0\,1\}$ faces. This is also not in agreement with the habits observed on natural and synthetic α-Al_2O_3 crystals. For the rutile crystal, according to the PBC theory [8], $\{1\,1\,0\}$ and $\{1\,0\,1\}$ are F forms; $\{0\,0\,1\}$ is S form. However, the $\{0\,0\,1\}$ faces easily appear on the synthetic rutile crystal [9] with the result that $\{0\,0\,1\}$ is incorrectly defined

* Corresponding author. Fax: + 86-21-599-27184.

0022-0248/00/$ - see front matter
PII: S0022-0248(99)00419-4

as S faces. In a previous paper [10], we presented the new rule of growth habit based on the study of the growth mechanism of oxide crystal. Its main contents include: (1) the growth rate of various faces is related to the element of which coordination polyhedron is present at the interface. The direction of the crystal face with the corner of the coordination polyhedron occurring at the interface has the fastest growth rate; the direction of the crystal face with the edge of the coordination polyhedron occurring at the interface the second fastest; the direction of the crystal face with the face of coordination polyhedron occurring at the interface the slowest. (2) The growth rate of various crystal faces is also related to the number of elements per coordination polyhedron present at the interface. The direction of the crystal face with more elements of the coordination polyhedron occurring at the interface has a faster growth rate. According to this new rule, the growth habits of ZnO and AlO(OH) crystals, and the habit change of ZnO crystalline particle had been explained reasonably. The aim of this paper is to explain the growth habits of α-Al_2O_3 and TiO_2 crystals observed under the hydrothermal conditions or the glycothermal conditions according to this new rule and the habit change of TiO_2 crystal by means of the study of its growth mechanism.

2. Experimental procedure

The reaction vessel adopted in the experiments is a silver-lined tube-type stainless steel autoclave about 215 ml capacity and 30 mm inner diameter. α-alumina was prepared using the newly prepared hydroxide colloids $Al(OH)_3$ as precursors by glycothermal method in 1,4-butanediol solution or by hydrothermal method in the mixed aqueous solution consisting of 0.5 mol/l KOH and 5 mol/l KBr. Aluminum hydrous oxide precursors were precipitated from 2 mol/l $Al(NO_3)_3 \cdot 9H_2O$ solution by slowly adding 1 mol/l KOH solution with rapid stirring of the aluminum-containing solution. TiO_2 powder was prepared by the hydrothermal method using $TiCl_4$ solution as precursors. The $TiCl_4$ solution with a certain concentration was obtained by the dilution of $TiCl_4$ in deionized water. The reaction temperature range from 200 to 350°C. After the hydrothermal or glycothermal treatment, the solid-reaction products were washed and filtered. The obtained powders are dried at 120°C for 24 h in air for X-ray diffraction measurements, ED analysis, and TEM or SEM morphological analyses.

3. Result and discussion

3.1. Growth habit of TiO_2 (rutile)

The TiO_2 powders are prepared by the hydrothermal method using $TiCl_4$ solution as the precursor at 200°C, 12 h. It was found that when the concentration of $TiCl_4$ solution is equal to 1 mol/l, the crystalline phases of prepared powders are rutile and anatase, in which the morphology of rutile is an elongated hexagonal prismatic form. Its TEM is shown in Fig. 1. In order to confirm the growth habit of rutile crystallite, the ED analysis of rutile crystallite is done. Its result is shown in Fig. 2. From Fig. 2, it can be obtained that the rutile crystallite is extended along the *c*-axis direction, and bounded by the {1 0 1}, {1 1 0} and {1 0 0} faces. Its growth habit is shown in Fig. 3.

According to the new rule concerning growth habit, the growth habit of a crystal is related to the orientation of the coordination polyhedron at the interface. Rutile belongs to the tetragonal crystal

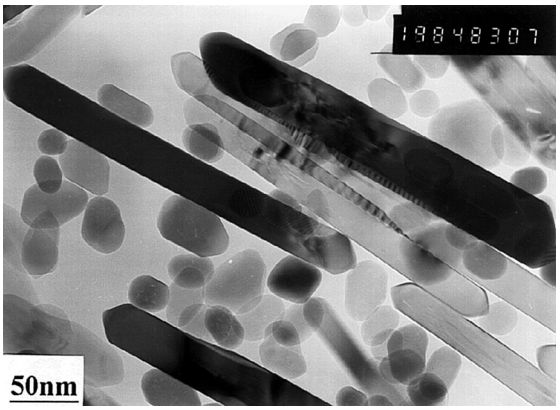

Fig. 1. TEM photograph of powders prepared by hydrothermal method using 1 mol/l $TiCl_4$ solution as precursor at 200°C.

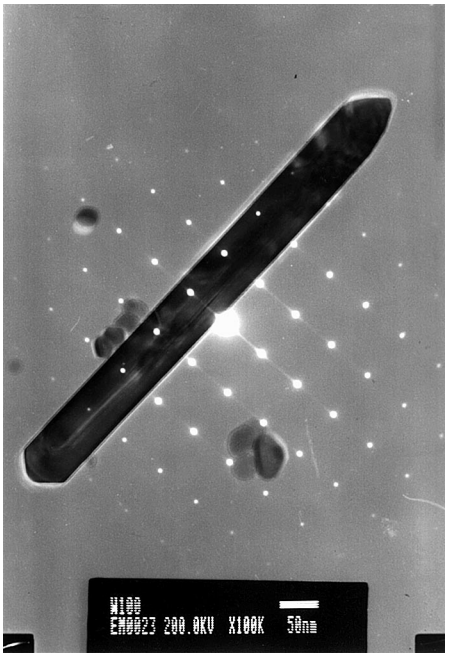

Fig. 2. ED pattern of powders prepared by hydrothermal method using 1 mol/l $TiCl_4$ solution as precursor at 200°C, 1 h.

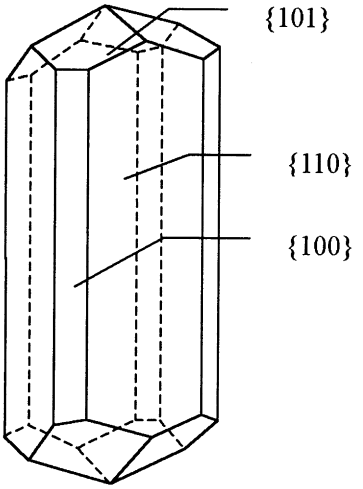

Fig. 3. Observed growth habit of TiO_2.

system. Its space group is D_{4h}^{14}-$p4_2/mnm$. The crystal lattice constants are $a_0 = 4.58$ Å, $c_0 = 2.95$ Å. Rutile has the HCP structure of oxygen anions. The structure consists of chains of TiO_6 octahedra, in

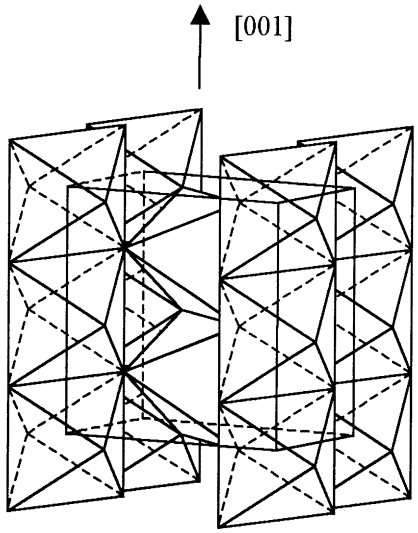

Fig. 4. Structure graph of TiO_2.

which each octahedron shares a pair of opposite edges, which are further linked by sharing vertices to form a 3D structure of 6 : 3 coordination. Its structure is shown in Fig. 4.

In Fig. 4, it can be seen that in the structure of TiO_2 crystal, there are two kinds of orientation of TiO_6 octahedra. For the $\{0\,0\,1\}$ faces, half of TiO_6 octahedra have two corners that appear at the interface while the others have no elements that appear at the interface. The number of corners per TiO_6 octahedra present at interface has an average of 1. However, for the other faces of TiO_2 crystal, in the steric structure diagram of crystal like Fig. 4, it is difficult to see clearly the orientation of TiO_6 octahedra at the interface due to the complicated structure of rutile. Hence, we adopt the projection of TiO_2 crystal structure as a medium to represent the orientation of TiO_6 octahedra at the interface. Fig. 5 show the projection of structure of TiO_2 along $[0\,0\,\bar{1}]$ direction.

In Fig. 5, it can be seen that for the prismatic form $\{1\,0\,0\}$, for half of TiO_6 octahedra, one corner and one edge appear at the interface while the others have no elements appearing at the interface. For the prismatic form $\{1\,1\,0\}$, half of the TiO_6 octahedra have one corner appearing at interface while the others have one edge which appears at interface. Therefore, for the prismatic form $\{1\,0\,0\}$

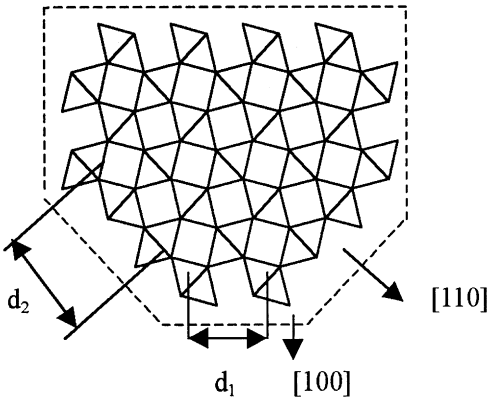

Fig. 5. Projection of structure of TiO_2 along $[0\,0\,\bar{1}]$ direction.

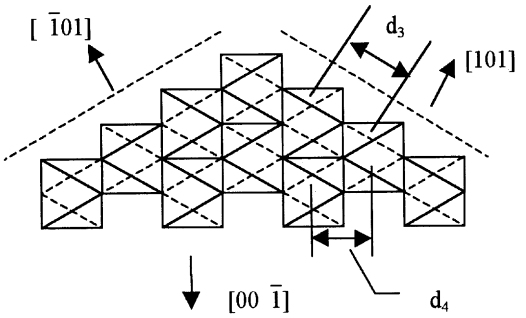

Fig. 6. Projection of structure of TiO_2 along $[0\,1\,0]$ direction.

and $\{1\,1\,0\}$, the number of corners per TiO_6 octahedra present at interface has an average of $\frac{1}{2}$. In Figs. 6 and 7, the projection of the structure of TiO_2 along $[0\,1\,0]$ and $[\bar{1}\,\bar{1}\,0]$ direction is shown, respectively.

In Fig. 6, it can be seen that at pyramidal form $\{1\,0\,1\}$, every TiO_6 octahedra has one corner occurring at the interface. In Fig. 7, it can be seen that at pyramidal form $\{1\,1\,1\}$, half of TiO_6 octahedra have two corners appearing at the interface while the other TiO_6 octahedra have one corner appearing at the interface. The number of corners per TiO_6 octahedra present at the interface has an average of $\frac{3}{2}$. From the analysis presented above, it can be shown that the relationship between the number (N) of corners per TiO_6 octahedra present and different crystal faces should be: $N_{\langle 1\,1\,0\rangle} = N_{\langle 1\,0\,0\rangle} < N_{\langle 1\,0\,1\rangle} = N_{\langle 0\,0\,1\rangle} < N_{\langle 1\,1\,1\rangle}$.

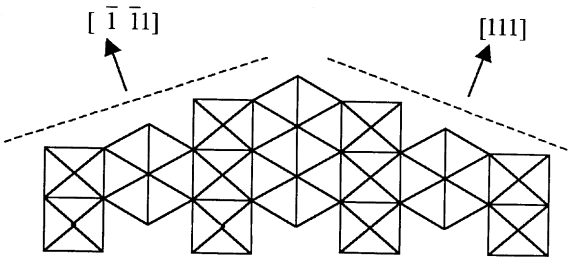

Fig. 7. Projection of structure of TiO_2 along $[\bar{1}\,\bar{1}\,0]$ direction.

According to the new rule concerning crystal growth habit, it can be deduced that the growth rate of $\{1\,1\,1\}$ faces is faster than that of $\{0\,0\,1\}$ or $\{1\,0\,1\}$ faces; the growth rate of $\{0\,0\,1\}$ or $\{1\,0\,1\}$ faces is faster than that of $\{1\,1\,0\}$ or $\{1\,0\,0\}$ faces.

Compared with the terminal vertex of edge or face of TiO_6 octahedra present at the interface, growth units easily link to the terminal vertex of corners of TiO_6 octahedra due to the bigger driving force on the terminal vertex of the corner. Hence, the more the number of the corners of TiO_6 octahedra present per unit area, the faster the growth rate of the crystal faces. For the $\{1\,1\,0\}$ and $\{1\,0\,0\}$ faces, although the average number of the corners per TiO_6 octahedra present at the interface is the same, the number of the corners of TiO_6 octahedra present per unit area is different. Thus, their growth rate can be compared by means of calculating the number of the corners of TiO_6 octahedra present per unit area. From Fig. 5, it can also be seen that for $\{1\,0\,0\}$ and $\{1\,1\,0\}$ faces, the distance between neighboring TiO_6 octahedra is different at the interface: $d_2/2 > d_1/2$, where $d_2/2$ is the distance between neighboring TiO_6 octahedra at interface of $\{1\,1\,0\}$ faces; $d_1/2$ is the distance between neighboring TiO_6 octahedra at interface of $\{1\,0\,0\}$ faces. Moreover, along the $[0\,0\,1]$ direction, the distance between neighboring TiO_6 octahedra is the same. So, although the average number of the corners per TiO_6 octahedra present at the interface is the same, the number of the corners of TiO_6 octahedra per unit area present at $\{1\,0\,0\}$ faces is greater than that at $\{1\,1\,0\}$ faces. According to the new rule concerning crystal growth habit, the growth rate of $\{1\,0\,0\}$ faces is faster than that of $\{1\,1\,0\}$ faces. In the same way, it can be obtained from Fig. 6 that the growth

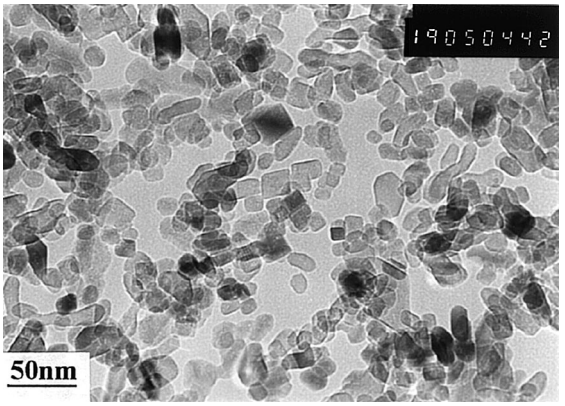

Fig. 8. TEM photograph of powders prepared by hydrothermal method using 0.25 mol/l $TiCl_4$ solution as precursor at 200°C, 12 h.

rate of $\{0\,0\,1\}$ faces is faster than that of $\{1\,0\,1\}$ faces because of $d_3 > d_4$, where d_4 is the distance between neighboring TiO_6 octahedra at $\{0\,0\,\bar{1}\}$ faces, d_3 is the distance between neighboring TiO_6 octahedra at $\{1\,0\,1\}$ faces. So, from the analysis presented above, it can be concluded that the relationship between the growth rate and different crystal faces is: $V_{\langle 1\,1\,0\rangle} < V_{\langle 1\,0\,0\rangle} < V_{\langle 1\,0\,1\rangle} < V_{\langle 0\,0\,1\rangle} < V_{\langle 1\,1\,1\rangle}$. So $\{0\,0\,1\}$ and $\{1\,1\,1\}$ faces easily disappear from the growth form. This result agrees with the observed growth habit by hydrothermal experiment.

Moreover, the growth habit of TiO_2 crystal is affected by the concentration of the $TiCl_4$ solution. When the concentration of $TiCl_4$ solution is equal to 0.25 mol/l, the crystalline phases of prepared powders consists of rutile and anatase. The morphology of rutile corresponds to prismatic form. Its TEM is shown in Fig. 8.

From the microscopy point of view, the formation mechanism of oxide crystals in aqueous solution mainly results from the formation mechanism of growth units and the incorporating mechanism of growth units into the crystal lattice at the interface. So, the formation mechanism of TiO_2 crystal under the hydrothermal condition can be represented as follows:

(1) The formation mechanism of growth units

$$Ti^{4+} + 4OH^- + 2H_2O = Ti(OH)_6^{2-} + 2H^+. \quad (1)$$

The incorporation mechanism of growth unit into crystal lattice by the dehydration reaction

$$Ti(OH)_6^{2-} + Ti(OH)_6^{2-} = Ti_2O(OH)_{10}^{4-} + H_2O, \quad (2)$$

$$\cdots\ \cdots$$

$$Ti_xO_y(OH)_z^{(z+2y-2x)-} + Ti(OH)_6^{2-} = Ti_{x+1}O_{y+1}(OH)_{z+4}^{(z+2y-2x+2)-} + H_2O. \quad (3)$$

$$\cdots\ \cdots$$

where the subscript x, y, z represents the numbers of Ti^{2+}, O^{2-}, OH^- within crystal, respectively.

So, it can be concluded that the growth rate of TiO_2 crystals is related to the formation rate of growth unit and the incorporating rate of growth unit into crystal lattice. The effects of the exterior condition on the growth rate of TiO_2 crystal are the result of its effect on the formation rate of growth unit. From Eq. (1), it can be seen that the formation rate of growth unit is related to the pH value of the reaction medium. When the pH value of the solution decreases, the growth rate of various faces decrease due to the smaller formation rate of the growth unit, but the difference of the growth rate of various faces increase. When the pH value of the solution decreases to a certain value, growth occurs only in the direction with the fastest growth rate, while the growth rate of other directions is almost equal to zero. Therefore, when the pH value of solution decreases, the morphology of powder is changed from prismatic to elongated prismatic form. The pH value of $TiCl_4$ solution is related to its concentration. When the concentration of $TiCl_4$ solution increases from 0.25 to 1 mol/l, the morphology of powders obtained is changed from shortened prismatic to elongated prismatic form due to the decrease of the pH value of $TiCl_4$ solution.

3.2. *Growth habit of α-Al_2O_3 crystal*

The hydrothermal method is normally used to study the growth habit of crystal because the supersaturation of solution is low during hydrothermal reaction. However, the minimum temperature at which α-Al_2O_3 forms in hydrothermal solution is about 400°C at high pressure, this temperature and pressure make fundamental studies on the growth

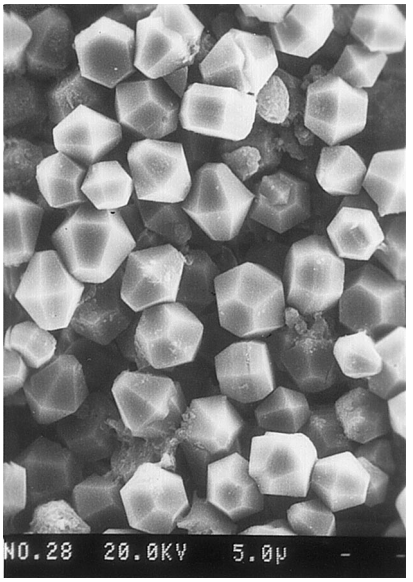

Fig. 9. SEM photograph of powder which is prepared by glycothermal treatment in 1,4-butanediol at 300°C, 12 h.

habit of α-Al_2O_3 crystal difficult. The crystalline temperature of α-Al_2O_3 crystal can be lowered by using KBr as an additive [11] or 1,4-butanediol solution as a reaction medium [12]. Fig. 9 shows the SEM photograph of α-Al_2O_3 powders that are prepared by glycothermal treatment in 1,4-butanediol at 300°C, 12 h. In Fig. 9, it can be seen that the growth habit of α-Al_2O_3 particles is platy $\{0\,0\,0\,1\}$, bounded by $\{0\,0\,0\,1\}$ and $\{1\,1\,\bar{2}\,3\}$ faces as shown in Fig. 10. Moreover, the growth habit of platy crystal bounded by $\{0\,0\,0\,1\}$ faces was also observed in the preparation of α-Al_2O_3 particles by hydrothermal crystalization using 5 mol/l KBr as an additive in 0.5 mol/l KOH solution at 350°C, 12 h. Its SEM photograph is shown in Fig. 11.

α-Al_2O_3 belongs to the trigonal crystal system; space group is D_6^{3d}-$R\bar{3}c$; the crystal lattice constants are $a_0 = 4.77$ Å, $c_0 = 13.04$ Å. The corundum structure is an approximate h.c.p. array of O atoms in which Al^{3+} ions occupy two-thirds of the octahedral holes. The coordination number of O is 4. The $[AlO_6]$ octahedrons constitute a layer by sharing edge, which is perpendicular to three-fold axis, as shown in Fig. 12a. At the direction parallel to three-fold axis, the hexagonal prism is formed by the

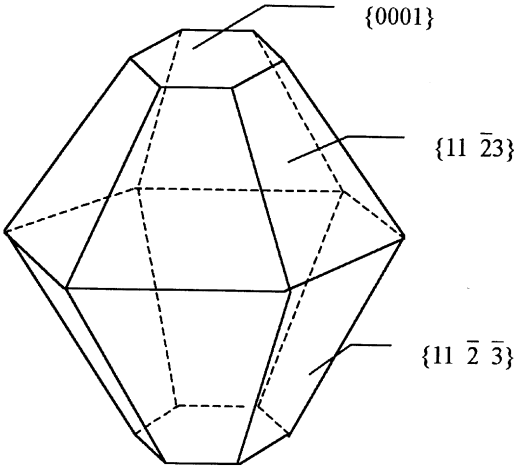

Fig. 10. Growth habit of α-Al_2O_3 crystal.

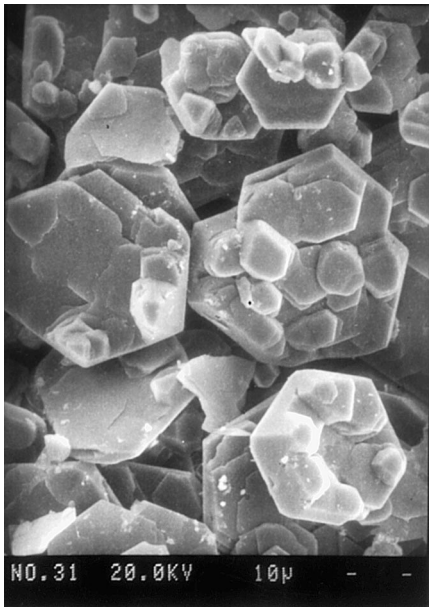

Fig. 11. SEM photograph of powder prepared by hydrothermal crystallization using 5 mol/l KBr as an additive in 0.5 mol/l KOH solution at 350°C, 12 h.

interval arrangement between two kinds of octahedrons: $[AlO_6]$ octahedrons which are stacked by sharing-face and hollow octahedrons which are surrounded by O^{2-}, as shown in Fig. 12b. Three-fold axis is formed by the linkage of $[AlO_6]$ octahedrons along c-axis, as shown in Fig. 12c.

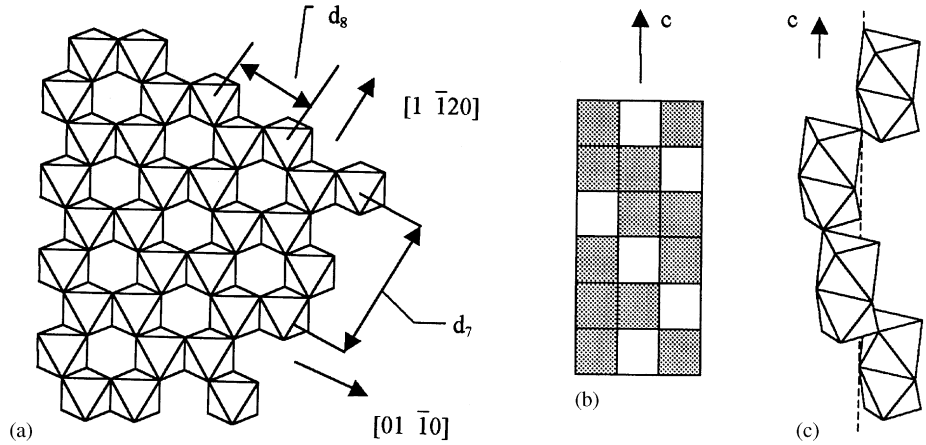

Fig. 12. Structure of α-Al_2O_3 crystal: (a) linkage mode of [AlO_6] octahedrons at (0 0 0 1) face, (b) arrangement mode of two kinds of octahedrons where black frame represents [AlO_6] octahedron, white frame represents hollow octahedron, and (c) linkage mode of [AlO_6] octahedrons along *c*-axis.

From Fig. 12a, it can be seen that for the $\{0\,1\,\bar{1}\,0\}$ faces, there are four corners of Al-O_6 octahedra present at the interface per space of d_7; there are two corners of Al-O_6 octahedra present at the interface of $\{1\,1\,\bar{2}\,0\}$ faces per space of d_8, and $d_7 = \sqrt{3}d_8 = \sqrt{3}a_0$. Moreover, the distance between neighboring Al-O_6 octahedra is the same along [0 0 0 1] direction. So, at $\{1\,1\,\bar{2}\,0\}$ faces, the number of corners of Al-O_6 octahedra present per unit area is $(2/a_0)/(4/\sqrt{3}a_0) = 0.866$ times that at $\{0\,\bar{1}\,1\,0\}$ faces. Figs. 13 and 14 shows the projection of the structure of α-Al_2O_3 along $[0\,1\,\bar{1}\,0]$, $[1\,\bar{1}\,2\,0]$ direction, respectively.

In Fig. 13, it can be seen that for the pyramidal faces $\{\bar{1}\,\bar{1}\,2\,3\}$, there are two corners of Al-O_6 octahedron present per space of d_5, where d_5 is the cyclic length at $\{\bar{1}\,\bar{1}\,2\,3\}$ faces consisting of three Al-O_6 octahedra. So, at $\{\bar{1}\,\bar{1}\,2\,3\}$ faces, there is an average of two-third of corners per Al-O_6 octahedra present at the interface. For the $\{1\,1\,\bar{2}\,0\}$ faces, there are two corners occurring at the interface in the space of d_6, where d_6 is the cyclic length along [0 0 0 1] direction consisting of three Al-O_6 octahedron. So, at $\{1\,1\,\bar{2}\,0\}$ faces, there is an average of two-third of corners per Al-O_6 octahedra present at the interface. Thus, at $\{\bar{1}\,\bar{1}\,2\,3\}$ and $\{1\,1\,\bar{2}\,0\}$ faces, every Al-O_6 octahedra has an average of two-thirds which is present at corners. However, although the average number of corners

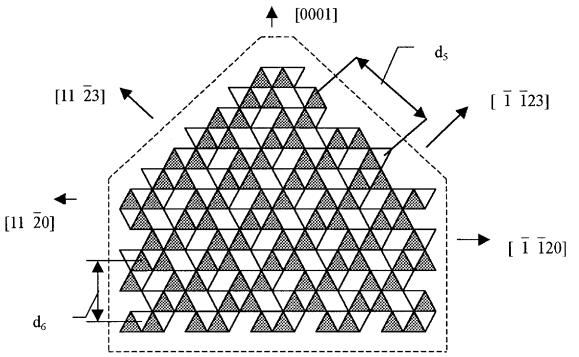

Fig. 13. Projection of the structure of α-Al_2O_3 along $[0\,1\,\bar{1}\,0]$ direction.

occurring at $\{1\,1\,\bar{2}\,0\}$ and $\{\bar{1}\,\bar{1}\,2\,3\}$ faces is the same, the number of corners of Al-O_6 octahedra present per unit area is different. From Fig. 13, it can be calculated that d_5 is equal to

$$\frac{\sqrt{(a_0/2)^2 + (c_0/3)^2}}{c_0/3} d_6 = 1.141 d_6$$

according to the index of $\{\bar{1}\,\bar{1}\,2\,3\}$ crystal face. Moreover, it can be seen from Fig. 12a that the space between the neighboring octahedra at the interface of $\{1\,1\,\bar{2}\,0\}$ and $\{\bar{1}\,\bar{1}\,2\,3\}$ faces along $[0\,1\,\bar{1}\,0]$ direction is equal to $d_8/2$. So, the number of Al-O_6 octahedra per unit area present at

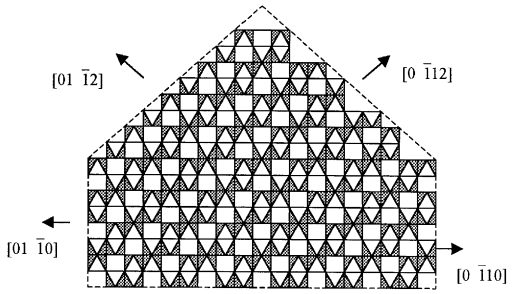

Fig. 14. Projection of the structure of α-Al_2O_3 along [1 $\bar{1}$ 2 0] direction.

$\{\bar{1}\,\bar{1}\,2\,3\}$ faces is $\frac{1}{1.141} = 0.876$ times that at $\{1\,1\,\bar{2}\,0\}$ faces. Thus, at the interface of $\{\bar{1}\,\bar{1}\,2\,3\}$ faces, the number of corners present per unit area is 0.876 times that at $\{1\,1\,\bar{2}\,0\}$ faces. In Fig. 13, it can also be seen that for $\{1\,1\,\bar{2}\,3\}$ faces, there are two kinds of interfaces of octahedra appearing during the growth of oxide crystals: consisting of an interface made up of Al-O_6 octahedra and an interface made up of hollow octahedra which is surrounded by O^{2-}, in which the ratio between interface of Al-O_6 octahedra and interface of hollow octahedra is 2 : 1. In addition, every Al-O_6 octahedron has one corner appearing at the interface made up of Al-O_6 octahedra. So, at the pyramidal faces $\{1\,1\,\bar{2}\,3\}$, there are an average of two-thirds corner of Al-O_6 octahedra present for every sites of octahedra in the interface. From the analysis presented above, it can be seen that at $\{\bar{1}\,\bar{1}\,2\,3\}$ faces, every Al-O_6 octahedra has an average of two-thirds which is present at corners. Moreover, it can be seen from Fig. 12a that the space between the neighboring octahedra at the interface of $\{1\,1\,\bar{2}\,3\}$ and $\{\bar{1}\,\bar{1}\,2\,3\}$ along [0 1 $\bar{1}$ 0] direction is equal to $d_8/2$. So, at the interface of $\{\bar{1}\,\bar{1}\,2\,3\}$ faces, the number of corners present per unit area is equal to that at the $\{1\,1\,\bar{2}\,3\}$ faces. In the same way, it can be deduced from Figs. 14 and 12a that at the interface of $\{0\,\bar{1}\,1\,0\}$ faces, the number of corners present per unit area is

$$\frac{\sqrt{(\sqrt{3}/2a_0)^2 + (c_0/2)^2}}{c_0/2} = 1.184$$

times that at $\{0\,\bar{1}\,1\,2\}$ faces. Namely, at the interface of $\{0\,\bar{1}\,1\,2\}$, the number of corners present per unit area is $\frac{1}{1.184} = 0.845$ times that at the interface of $\{0\,\bar{1}\,1\,0\}$ faces. Moreover, it can also be deduced from Figs. 14 and 12a that at the $\{0\,1\,\bar{1}\,2\}$ interface, the number of corners present per unit area is equal to that at the $\{0\,\bar{1}\,1\,2\}$ faces. From the above presented analysis, it can be derived that at $\{1\,1\,\bar{2}\,0\}$ faces, the number of corners of Al-O_6 octahedra present per unit area is 0.866 times that at $\{0\,\bar{1}\,1\,0\}$ interface; at $\{\bar{1}\,\bar{1}\,2\,3\}$ interface, the number of corners present per unit area is 0.876 times that at $\{1\,1\,\bar{2}\,0\}$ faces. So, at $\{\bar{1}\,\bar{1}\,2\,3\}$ interfaces, the number of corners present per unit area is $0.866 \times 0.845 = 0.759$ times that at $\{0\,\bar{1}\,1\,0\}$ faces. Thus, the relationship between the number (N) of corners per unit area present and different crystal faces is: $N_{\langle 1\,1\,\bar{2}\,3\rangle} = N_{\langle \bar{1}\,\bar{1}\,2\,3\rangle} = 0.759N_{\langle 0\,\bar{1}\,1\,0\rangle}$; $N_{\langle 0\,1\,\bar{1}\,2\rangle} = N_{\langle 0\,\bar{1}\,1\,2\rangle} = 0.845N_{\langle 0\,\bar{1}\,1\,0\rangle}$; $N_{\langle 1\,1\,\bar{2}\,0\rangle} = 0.866N_{\langle 0\,\bar{1}\,1\,0\rangle}$; $N_{\langle 0\,1\,\bar{1}\,0\rangle} = N_{\langle 0\,\bar{1}\,1\,0\rangle}$. According to the new rule of growth habit, the relationship between the velocities of crystal growth and different directions should be: $V_{\langle 1\,1\,\bar{2}\,3\rangle} = V_{\langle \bar{1}\,\bar{1}\,2\,3\rangle} < V_{\langle 0\,1\,\bar{1}\,2\rangle} = V_{\langle 0\,\bar{1}\,1\,2\rangle} < V_{\langle 1\,1\,\bar{2}\,0\rangle} < V_{\langle 0\,1\,\bar{1}\,0\rangle} = V_{\langle 0\,\bar{1}\,1\,0\rangle}$. Moreover, it can be seen from Fig. 12a that at the $\{0\,0\,0\,1\}$ faces, every Al-O_6 octahedra has a face occurring at the interface, so the growth rate of the $\{0\,0\,0\,1\}$ faces is the slowest. Thus, the following relationship between the velocities of crystal growth and different directions should be: $V_{\langle 0\,0\,0\,1\rangle} < V_{\langle 1\,1\,\bar{2}\,3\rangle} = V_{\langle \bar{1}\,\bar{1}\,2\,3\rangle} < V_{\langle 0\,1\,\bar{1}\,2\rangle} = V_{\langle 0\,\bar{1}\,1\,2\rangle} < V_{\langle 1\,1\,\bar{2}\,0\rangle} < V_{\langle 0\,1\,\bar{1}\,0\rangle} = V_{\langle 0\,\bar{1}\,1\,0\rangle}$. So, $\{0\,0\,0\,1\}$ and $\{1\,1\,\bar{2}\,3\}$ faces appear easily. This is consistent with the growth habit of α-Al_2O_3 crystal particles resulting from hydrothermal experiment.

4. Conclusions

The growth habit of α-Al_2O_3 and rutile crystal, and the habit change of rutile are successfully explained by the new rule concerning growth habit. The main results are:

(1) The growth habit of α-Al_2O_3 is platy $\{0\,0\,0\,1\}$, not rhombohedral $\{\bar{1}\,0\,1\,2\}$. Its relationship of growth rate of various faces is: $V_{\langle 0\,0\,0\,1\rangle} < V_{\langle 1\,1\,\bar{2}\,3\rangle} < V_{\langle 0\,1\,\bar{1}\,2\rangle} = V_{\langle 0\,\bar{1}\,1\,2\rangle} < V_{\langle 1\,1\,\bar{2}\,0\rangle}$

$< V_{\langle 0\,1\,\bar{1}\,0\rangle} = V_{\langle 0\,\bar{1}\,1\,0\rangle}$. This result is in good agreement with the observed results by hydrothermal experiment.

(2) The growth habit of rutile is elongated prismatic form. The importance of growth habit of rutile crystal decrease in the order of $\{1\,1\,0\} > \{1\,0\,0\} > \{1\,0\,1\} > \{0\,0\,1\} > \{1\,1\,1\}$. This result agrees with the observed growth habit on the crystal obtained from hydrothermal crystallization using 1 mol/l $TiCl_4$ solution as precursor at 200°C.

(3) The morphology of TiO_2 crystalline particles prepared at 200°C is related to the concentration of $TiCl_4$ solution, and becomes elongated as the concentration of $TiCl_4$ solution increases from 0.25 to 1 mol/l. The growth habit change of TiO_2 crystal is explained by the study of its growth mechanism in hydrothermal solution.

Acknowledgements

The authors thank Professor S.R. Coriell for the detailed revision of the poor English in the manuscript. This project is supported by National Science Foundation of China (Grant No. 59832080, 59772002).

References

[1] J.D.H. Donnay, D. Harker, Amer. Mineral 22 (1937) 446.
[2] P. Hartman, W.G. Perdok, Acta Crystallogr. 8 (1955) 525.
[3] P. Hartman, Zap. Vses. Mineral Obshch. 91 (1962) 672.
[4] P. Hartman, J. Crystal Growth 96 (1989) 667.
[5] P. Hartman, J. Crystal Growth 49 (1980) 166.
[6] K. Watanabe, J. Crystal Growth 65 (1983) 568.
[7] W.C. Mackrodt, R.J. Davey, S.N. Black, J. Crystal Growth 80 (1987) 441.
[8] P. Hartman (Ed.), Crystal Growth: An Introduction, North-Holland, Amsterdam, London, pp. 384–385.
[9] Peter M. Oliver, Graeme W. Watson, E. Toby Kelsey, Stephen C. Parker, Mater. Chem. 7 (3) (1997) 563.
[10] W.J. Li, E.-W. Shi, W.-Z. Zhong, J. Crystal Growth (1999), in preparation.
[11] Seung Beom Cho, Sridhar Venigalla, James H. Adair, J. Am. Ceram Soc. 79 (1) (1996) 88.
[12] M.V. Danthevskaya, USSR, Patent SU14771, 682 (CL. CO IF 7/02), 7 May 1989.